

cathode can then be used to machine electrochemically the workpiece. In short, the main advantages of ECM are:

- (i) the rate of metal machining does not depend on the hardness of the metal;
- (ii) complicated shapes can be machined on hard metals;
- (iii) there is no tool wear.

### Bibliography

- Faraday, M., *Experimental Researches in Electricity*, Vols. I, II, III, reprinted by Dover, New York (1965).  
Glasstone, S., *The Elements of Physical Chemistry*, Macmillan, London (1950).  
Gusseff, W., British Patent No. 335 003.  
Hadfield, R. A., *Faraday and His Metallurgical Researches*, Chapman and Hall, London (1931).

## CHAPTER TWO

### **Basic Fluid Dynamics**

In the first chapter, the need for electrolyte flow in ECM was established. An understanding of the fluid dynamics involved in the process can be obtained from the analysis of five basic equations, which describe the likely patterns of the flow. In particular, these equations provide a guide to the significance of flow velocity profiles. From such studies the pressures can be estimated that are required to pump the electrolyte at specific rates down the gap between the two electrodes, and useful information can be obtained about the variation in electrolyte velocity *across* the gap.

In the treatment of such matters in this chapter emphasis is given to flow along rectangular channels and circular pipes since these flow channels are common in ECM. Nevertheless, the principles which are discussed are applicable also to other flow configurations, such as those arising with the rotating disc. The use of that type of configuration in both fluid dynamics and electrochemical (including ECM) studies is well known [1, 2].

#### 2.1 Basic assumptions and definitions

Investigations concerned with real, as distinct from perfect, fluid motion rely heavily on two assumptions. The first is that, wherever the fluid is in contact with a solid boundary, there is no motion or slip, relative to that boundary, of the fluid particles adjacent to it. In the second assumption, the shearing (i.e. tangential) stress between adjacent layers of fluid of infinitesimally small thickness is taken to be proportional to the rate of shear in the direction perpendicular

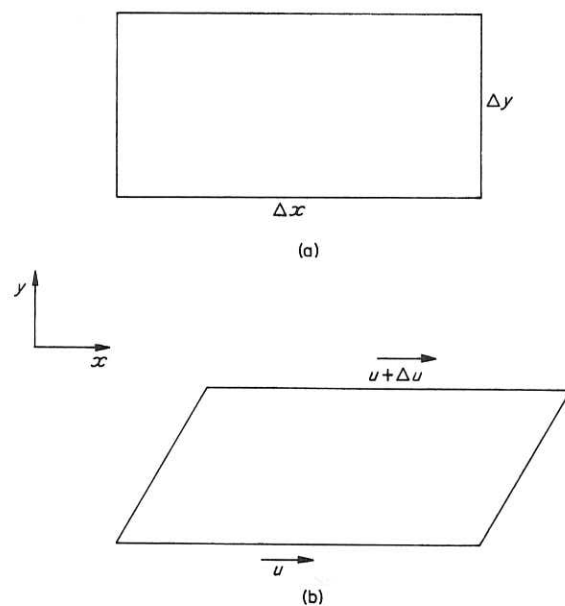


Fig. 2.1 Particle of viscous fluid set in motion

to the motion. Thus, consider a fluid particle, as shown in Fig. 2.1(a), whose sides are  $\Delta x$  and  $\Delta y$ . If it is set in motion in the  $x$  direction with a velocity  $u$  on its lower surface and  $u + \Delta u$  on the upper surface, its shape will change to that shown in Fig. 2.1(b). The rate of shear in the direction normal to the motion is then  $\Delta u/\Delta y$ , so that the limiting value of the rate of shear for an infinitesimally small particle is  $\partial u/\partial y$ . Use of the second assumption for the shearing stress  $\tau$  at any point leads to the equation

$$\tau = \mu \frac{\partial u}{\partial y}$$

where  $\mu$  is a coefficient of proportionality, usually termed the absolute viscosity of the fluid. A fluid which obeys such a relationship is known as a Newtonian fluid. ECM electrolytes, water, air, and gases can all be regarded as Newtonian.

Thus

$$\mu = \tau / \left( \frac{\partial u}{\partial y} \right) \quad (2.1)$$

That is, the viscosity is the ratio of shear stress to transverse velocity gradient.

#### (a) Kinematic viscosity

It is often convenient to deal with the kinematic viscosity,  $\nu$ , obtained by dividing  $\mu$  by the density,  $\rho_e$ , of the fluid:

$$\nu = \frac{\mu}{\rho_e} \quad (2.2)$$

#### (b) Specific viscosity

This is defined as ratio of the absolute viscosity of the fluid to that of water at 20°C.

The viscosity of water at 20°C is almost 1 cP so that the viscosity in centipoise is numerically equal to the specific viscosity. For liquids,  $\mu$  is nearly independent of pressure and decreases rapidly as the temperature increases;  $\nu$  has the same dependence. The liquid electrolytes used in ECM, of course, obey these conditions. A particular requirement for them is that their viscosity should be low, so that they can be pumped at high rates down the inter-electrode gap without the need for excessively high pump pressures. For example, for 10% (w/w) NaCl solution in water,  $\mu = 1.23$  cP at 18°C; at 40°C,  $\mu = 0.78$  cP. Since  $\rho_e = 1.07$  g/cm<sup>3</sup> at 18°C and 1.06 g/cm<sup>3</sup> at 40°C, the corresponding  $\nu$  values are 1.15 mm<sup>2</sup>/s and 0.735 mm<sup>2</sup>/s respectively. For gases,  $\mu$  increases with temperature, although it is again independent of pressure;  $\nu$  increases rapidly with temperature since the density decreases rapidly with increasing temperature.

#### (c) Compressibility

Compressibility gives a measure of the change of volume of a fluid subjected to normal pressures or tensions. It can be defined thus: compressibility = percentage change in volume for a given pressure change.

For water, a pressure increase of 101 kN/m<sup>2</sup> causes a relative change in volume of about 0.005%. This low value is typical of most liquids, so that they may be regarded as incompressible. Air, however, at NTP is about 20 000 times more compressible than water. This is typical for most gases. In the work which follows we shall

assume that the fluid is incompressible, and consider implicitly that it is an electrolyte.

(d) *Reynolds number*

The dimensionless quantity

$$\rho_e \frac{Ul}{\mu} = \frac{Ul}{\nu} = Re \quad (2.3)$$

where  $l$  and  $U$  are a characteristic length and velocity, respectively, for the flow path, is termed the Reynolds number,  $Re$ .

(e) *Hydraulic diameter*

In ECM, the electrolyte often flows through channels of non-circular cross-section. It is convenient then to define a 'hydraulic diameter',  $d_h$ ,

$$d_h = \frac{4A}{C} \quad (2.4)$$

where  $A$  is the cross-section area and  $C$  is the wetted perimeter.

For a rectangular flow channel, formed by plane, parallel electrodes, where the gap  $h$  is much smaller than the electrode width,  $b$

$$d_h = 4bh/2(b+h) \approx 2h \quad (2.5)$$

## 2.2 Navier-Stokes equations

The flow of a viscous fluid like an electrolyte can be specified by the three orthogonal components ( $u, v, w$ ) of its velocity  $U$ , the pressure  $p(x, y, z, t)$ , and density  $\rho_e(x, y, z, t)$ , where  $x, y, z$  are the usual orthogonal coordinates of position and  $t$  is the time. Five equations are available for the determination of  $u, v, w, p$ , and  $\rho_e$ . They are (i) the three equations of motion for the conservation of momentum, (ii) the continuity equation for the conservation of mass, and (iii) the thermodynamic equation of state.

The equations of motion are obtained from Newton's second law. In the application of this law to a fluid in motion, two types of forces must be considered: (a) body (e.g. gravitational) forces, which act throughout the mass of the body, and (b) pressure and friction

forces, which act on its boundary. The equations of motion can then be expressed in the form

$$\rho_e \frac{dU}{dt} = F + P \quad (2.6)$$

where  $F$  is the gravitational force per unit volume ( $\rho_e g$ ,  $g$  being the acceleration due to gravity) and  $P$  is the boundary force. As usual,  $F$  and  $P$  can be written in component form:

$$F = iF_x + jF_y + kF_z \quad (2.7)$$

and

$$P = iP_x + jP_y + kP_z \quad (2.8)$$

where  $i, j$ , and  $k$  are unit vectors along the  $x, y$ , and  $z$  axes. It should be noted that these are the only types of forces considered in this analysis. Little is yet known about the effect on the fluid motion of other forces that may arise in ECM, for instance, those of an electromagnetic nature.

The thermodynamic equation of state can be shown to have the form

$$F(\rho, p, T) = 0 \quad (2.9)$$

For instance, for a perfect gas, the usual equation of state is

$$p = \rho_g RT \quad (2.10)$$

where  $\rho_g$  is the gas density,  $R$  is the gas constant, and  $T$  the temperature.

Discussion of these equations is available elsewhere [1]. Since we are mainly concerned with liquid electrolytes, it is sufficient for our purposes to write down the fundamental equations of motion for incompressible flow:

$$\rho_e \left( \frac{\partial u}{\partial t} + u \frac{\partial u}{\partial x} + v \frac{\partial u}{\partial y} + w \frac{\partial u}{\partial z} \right) = F_x - \frac{\partial p}{\partial x} + \mu \left( \frac{\partial^2 u}{\partial x^2} + \frac{\partial^2 u}{\partial y^2} + \frac{\partial^2 u}{\partial z^2} \right) \quad (2.11)$$

$$\rho_e \left( \frac{\partial v}{\partial t} + u \frac{\partial v}{\partial x} + v \frac{\partial v}{\partial y} + w \frac{\partial v}{\partial z} \right) = F_y - \frac{\partial p}{\partial y} + \mu \left( \frac{\partial^2 v}{\partial x^2} + \frac{\partial^2 v}{\partial y^2} + \frac{\partial^2 v}{\partial z^2} \right) \quad (2.12)$$

$$\rho_e \left( \frac{\partial w}{\partial t} + u \frac{\partial w}{\partial x} + v \frac{\partial w}{\partial y} + w \frac{\partial w}{\partial z} \right) = F_z - \frac{\partial p}{\partial z} + \mu \left( \frac{\partial^2 w}{\partial x^2} + \frac{\partial^2 w}{\partial y^2} + \frac{\partial^2 w}{\partial z^2} \right) \quad (2.13)$$

$$\frac{\partial u}{\partial x} + \frac{\partial v}{\partial y} + \frac{\partial w}{\partial z} = 0 \quad (2.14)$$

The first three equations are the Navier-Stokes equations. The fourth is the equation of continuity.

### 2.3 Laminar flow

In ECM the flow is likely to be either *laminar* or *turbulent*, although the latter will be shown later to be more common. In laminar flow, agitation of the fluid particles is of a molecular nature, and these particles are constrained to motion in parallel paths, or layers, by the action of viscosity. The shearing stress between adjacent moving layers is determined by the viscosity, and is defined by Equation (2.1). Some characteristic behaviour can be obtained from an examination of laminar flow down a straight channel.

#### 2.3.1 Laminar flow down a straight channel

Consider two-dimensional, steady, laminar flow down a straight channel with parallel flat walls, spaced distance  $h$  apart. Since the flow is steady, all time derivatives of the velocity are zero. If the flow is also assumed to be parallel in the  $x$  direction so that there is only one velocity component, the equation of continuity (2.14) gives that

$$\frac{\partial u}{\partial x} = 0$$

Then

$$u = u(y) \quad \text{and} \quad \frac{\partial^2 u}{\partial x^2} = 0$$

$$v = 0$$

$$w = 0$$

From the equations of motion (2.12) and (2.13) for the  $y$  and  $z$  directions,

$$\frac{\partial p}{\partial y} = \frac{\partial p}{\partial z} = 0; \quad \frac{\partial p}{\partial x} = \text{constant.}$$

The Navier-Stokes equation (2.11) for the  $x$  direction then becomes

$$\frac{dp}{dx} = \mu \frac{d^2 u}{dy^2} \quad (2.15)$$

The solution to Equation (2.15) is

$$u = \frac{1}{2\mu} \left( -\frac{dp}{dx} \right) \left( \frac{h^2}{4} - y^2 \right) \quad (2.16)$$

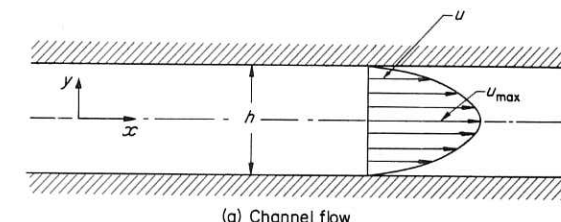
the boundary conditions being  $u = 0$  at  $y = \pm h/2$ . The maximum velocity,  $u_{\max}$ , is given by

$$u_{\max} = \frac{h^2}{8\mu} \left( -\frac{dp}{dx} \right) \quad (2.17a)$$

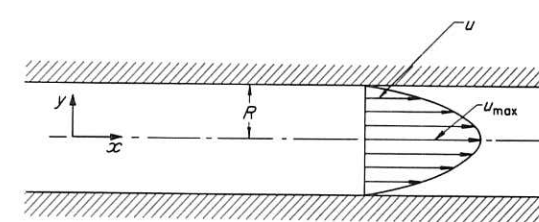
whilst the average velocity  $\bar{u}$  is

$$\begin{aligned} \bar{u} &= \frac{2}{3} u_{\max} \\ &= \frac{h^2}{12\mu} \left( -\frac{dp}{dx} \right) \end{aligned} \quad (2.17b)$$

From Equation (2.16), the velocity distribution is deduced to be parabolic. This type of velocity profile, which is shown in Fig. 2.2, is a characteristic of laminar flow.



(a) Channel flow



(b) Pipe flow

Fig. 2.2 Parabolic velocity distribution for laminar flow

#### 2.3.2 Hagen-Poiseuille flow

The above analysis on flow down a channel can be extended to cover steady laminar flow due to a pressure drop along a straight pipe of

circular cross-section. This is usually termed Hagen–Poiseuille flow. The velocity distribution may be obtained by putting the Navier–Stokes equations into cylindrical coordinates. The equations then reduce to one equation for the  $x$  direction (taken to be coincident with the axis of the pipe). Since the tangential and radial velocity components are zero, the velocity component in the  $x$  direction depends only on  $y$ , and the pressure gradient  $dp/dx$  is constant. The equation can be written:

$$\frac{dp}{dx} = \mu \left( \frac{d^2 u}{dy^2} + \frac{1}{y} \frac{du}{dy} \right)$$

where  $u = 0$  at  $y = R$ ,  $R$  being the radius of the pipe. The solution is

$$u(y) = -\frac{1}{4\mu} \frac{dp}{dx} (R^2 - y^2)$$

Here, the constant pressure gradient,  $-(dp/dx) = (p_1 - p_2)/L$ , is assumed to be known,  $L$  being the pipe length.

As before, the maximum velocity  $u_{\max}$  can be calculated:

$$u_{\max} = \frac{R^2}{4\mu} \left( -\frac{dp}{dx} \right) \quad (2.18)$$

whilst the mean velocity  $\bar{u}$  is

$$\begin{aligned} \bar{u} &= \frac{1}{2} u_{\max} \\ &= \frac{R^2}{8\mu} \left( -\frac{dp}{dx} \right) \end{aligned} \quad (2.19)$$

This equation, and that above for flow down a channel, Equation (2.17b), are used to calculate the pressure difference required to overcome viscous forces in laminar flow.

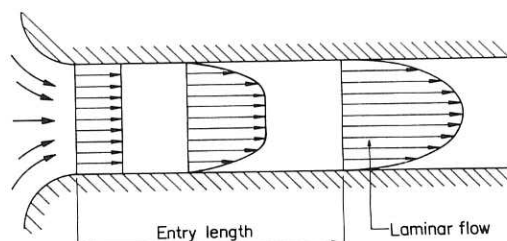


Fig. 2.3 Establishment of fully developed laminar flow

Note that in Sections 2.3.1 and 2.3.2, the average velocity can be expressed in terms of the volumetric flow-rate  $Q$ , the flow quantity usually measured in ECM. For instance, in pipe flow,  $Q = \pi R^2 \bar{u}$ .

In the above analyses, the laminar flow has been assumed to be fully developed. This condition is only achieved at some distance from the entrance to the channel. In Fig. 2.3, it is seen that the velocity distribution in a pipe can change from an almost uniform profile at the smoothly curved inlet to a fully developed profile further downstream. The transition is caused by an increase in viscous effects along the channel. The entry length,  $x_E$ , required for fully developed flow was established theoretically by Boussinesq as

$$x_E = 0.03 d \text{Re} \quad (2.20)$$

where  $d$  is the pipe diameter and  $\text{Re}$  the Reynolds number ( $= \bar{u}d/\nu$ ). Thus, for  $\text{Re} = 1000$ ,  $x_E$  is about 30 pipe diameters. [No equivalent formula to (2.20) exists for turbulent flow, although experiments have shown that  $x_E$  is often about 50 to 100 diameters.]

From the discussion of ‘internal’ flow in channels and pipes, we move to considerations of flow around objects, or ‘external’ flow. Although the latter flow can be described by the same equations of motion used for internal flow, its characteristics are quite different. A typical example of external flow is flow over a flat plate. Closely associated with this kind of flow is the phenomenon of boundary layers.

## 2.4 Boundary layers in laminar flow

### 2.4.1 Thickness of laminar boundary layer

For an electrolyte, flowing over a rigid body (for example, a flat plate), the ‘no slip’ condition applies at the surface of the body. That is, the fluid velocity at that surface is zero. Experiments show that the fluid velocity increases from zero at the boundary to its mainstream value over a thin layer, termed the ‘boundary layer’. Over the boundary layer, the fluid velocity gradient is high, and viscous effects have as much influence as inertia effects. Outside the layer, the velocity gradients and the viscous shear are small. The flow is then influenced by inertia, pressure gradient, and body forces. The importance of the boundary layer in ECM will become apparent in later chapters. At this stage it is useful to obtain an expression for its magnitude,  $\delta_0$ .

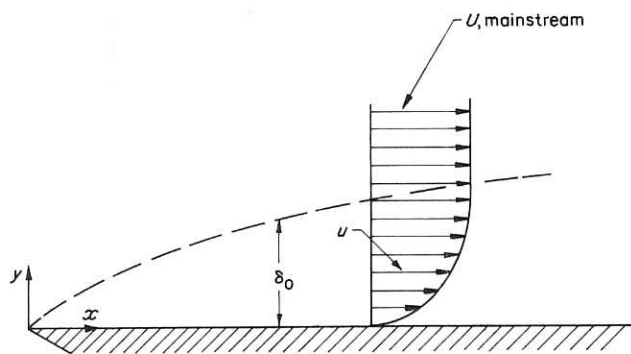


Fig. 2.4 Velocity distribution in the boundary layer

Let us examine the Navier-Stokes equations for the boundary layer for two-dimensional, steady incompressible flow over a flat plate (Fig. 2.4). Since body forces can be ignored, then, from Equations (2.11) and (2.12):

$$\rho_e \left( u \frac{\partial u}{\partial x} + v \frac{\partial u}{\partial y} \right) = - \frac{\partial p}{\partial x} + \mu \left( \frac{\partial^2 u}{\partial x^2} + \frac{\partial^2 u}{\partial y^2} \right) \quad (2.21)$$

$$\rho_e \left( u \frac{\partial v}{\partial x} + v \frac{\partial v}{\partial y} \right) = - \frac{\partial p}{\partial y} + \mu \left( \frac{\partial^2 v}{\partial x^2} + \frac{\partial^2 v}{\partial y^2} \right) \quad (2.22)$$

The continuity equation (2.14) reduces to

$$\frac{\partial u}{\partial x} + \frac{\partial v}{\partial y} = 0 \quad (2.23)$$

Let us now carry out a rough order of magnitude study of the terms in the above equations. First it is noted that, since  $\delta_0/x$  is usually very small, the boundary layer is thin,  $x$  being a distance measured from the leading edge of the plate. A time scale is now chosen so that  $U$ , the mainstream velocity, is the same order of magnitude as  $x$ . Suppose, too, that  $x$  is of order unity. We write

$$U \approx x = O(1)$$

Now magnitudes of distances in the  $y$  direction within the boundary layer are much less than  $x$ . These are denoted by  $O(\delta_0)$ . That is

$$O(\delta_0) \ll O(1)$$

The extreme value of the difference of the velocity  $u$  in the  $y$  direction is also  $O(1)$ , since this velocity goes from zero to  $U$ . This condition also holds for the second difference of  $u(y)$ . Since the extreme difference of  $y$  is  $O(\delta_0)$ ,

$$\frac{\partial u}{\partial y} = O\left(\frac{1}{\delta_0}\right)$$

$$\frac{\partial^2 u}{\partial y^2} = O\left(\frac{1}{\delta_0^2}\right)$$

Next,  $u$  can change from almost  $U$  at  $x = 0$  to almost zero at  $x$ . Thus the extreme magnitude of  $\partial u / \partial x$  is unity. Then

$$\frac{\partial u}{\partial x} = O(1)$$

Similarly,

$$\frac{\partial^2 u}{\partial x^2} = O(1)$$

The continuity equation (2.14) shows that since  $\partial u / \partial x$  is  $O(1)$ , so must be  $\partial v / \partial y$ . Since changes in  $y$  are  $O(\delta_0)$ , changes in  $v(y)$  are also  $O(\delta_0)$ . Finally, since  $v = 0$  for  $y = 0$ ,  $v = O(\delta_0)$ . We may now write

$$v = O(\delta_0)$$

$$\frac{\partial v}{\partial y} = O(1)$$

$$\frac{\partial^2 v}{\partial y^2} = O\left(\frac{1}{\delta_0}\right)$$

$$\frac{\partial v}{\partial x} = O(\delta_0)$$

$$\frac{\partial^2 v}{\partial x^2} = O(\delta_0)$$

In the original equation (2.21) we then have

$$\begin{aligned} u \frac{\partial u}{\partial x} + v \frac{\partial u}{\partial y} &= - \frac{1}{\rho_e} \frac{\partial p}{\partial x} + \frac{\mu}{\rho_e} \left( \frac{\partial^2 u}{\partial x^2} + \frac{\partial^2 u}{\partial y^2} \right) \\ [O(1)][O(1)] + [O(\delta_0)][O(1/\delta_0)] &= - \frac{1}{\rho_e} \frac{\partial p}{\partial x} + \frac{\mu}{\rho_e} ([O(1)] + [O(1/\delta_0^2)]) \end{aligned} \quad (2.24)$$

Since terms of  $O(1)$  are much less than terms of  $O(1/\delta_0^2)$ ,  $\partial^2 u/\partial x^2$  can be neglected in comparison with  $\partial^2 u/\partial y^2$ .

But the expression  $(\partial^2 u/\partial x^2 + \partial^2 u/\partial y^2)$  is derived from friction effects which are considerable in the boundary layer. It must, therefore, have an order of magnitude similar to those of the other expressions in Equation (2.24). Those expressions have an order of magnitude of unity. Thus

$$\nu[O(1/\delta_0^2)] = O(1)$$

where  $\mu/\rho_e = \nu$ , the kinematic viscosity. Accordingly,

$$\nu = O(\delta_0^2)$$

Note, too, that a Reynolds number  $Re$  of the form  $Ux/\nu$  is of order  $O(1/\delta_0^2)$ . That is,  $\delta_0$  is related to  $Re$  by

$$\delta_0 = O(Re^{-1/2})$$

and since  $x$  is of order of magnitude unity,

$$\frac{\delta_0}{x} = O(Re^{-1/2})$$

Insertion of the experimentally and theoretically derived, numerical coefficient gives the result:

$$\delta_0 = 5 \left( \frac{\nu x}{U} \right)^{1/2} \quad (2.25)$$

This equation describes the distance from the wall at which the boundary layer has sensibly merged with the mainstream.

#### 2.4.2 Prandtl's boundary layer equations

Consider the second of the Navier-Stokes equations (2.12) and the corresponding order of magnitude:

$$u \frac{\partial v}{\partial x} + v \frac{\partial v}{\partial y} = - \frac{1}{\rho_e} \frac{\partial p}{\partial y} + \nu \left( \frac{\partial^2 v}{\partial x^2} + \frac{\partial^2 v}{\partial y^2} \right)$$

$$[O(1)][O(\delta_0)] + [O(\delta_0)][O(1)] = - \frac{1}{\rho_e} \frac{\partial p}{\partial y} + [O(\delta_0^2)][O(\delta_0)] + O(1/\delta_0) \quad (2.26)$$

Note that  $\partial^2 v/\partial x^2$  is negligible compared with  $\partial^2 v/\partial y^2$ . Since the term  $[-(1/\rho_e)(\partial p/\partial y)]$  is significant, it will be  $O(\delta_0)$ . Now  $\rho_e$  can be taken to be  $O(1)$  or less, thus  $\partial p/\partial y$  is  $O(\delta_0)$ . It is also clear that

the velocity  $v$  which is  $O(\delta_0)$  is negligible compared with  $u$ , which is  $O(1)$ . We thus can neglect Equation (2.26) on the basis of an effectively constant pressure through the boundary layer. Then we consider only the previous equation (2.24) with  $\partial^2 u/\partial x^2$  deleted. That is

$$u \frac{\partial u}{\partial x} + v \frac{\partial u}{\partial y} = - \frac{1}{\rho_e} \frac{\partial p}{\partial x} + \nu \frac{\partial^2 u}{\partial y^2} \quad (2.27)$$

$$\frac{\partial u}{\partial x} + \frac{\partial v}{\partial y} = 0 \quad (2.28)$$

Equations (2.27) and (2.28) are known as Prandtl's boundary layer equations for steady flow.

#### 2.4.3 Bernoulli's equation

Near the outer edge of the boundary layer,  $u = U$ . Over this region there is no large velocity gradient and the viscous terms in Equation (2.27) can be ignored. We obtain

$$U \frac{\partial U}{\partial x} = - \frac{1}{\rho_e} \frac{\partial p}{\partial x} \quad (2.29)$$

Integration gives

$$p + \frac{1}{2} \rho_e U^2 = \text{constant} \quad (2.30)$$

This is Bernoulli's equation, from which the pressure required to overcome inertia can be calculated.

#### 2.5 Transition from laminar to turbulent flow

From the Hagen-Poiseuille equation, we have seen that the velocity distribution for laminar flow is parabolic. The usual criterion for the existence of laminar flow down a pipe of diameter  $d$  is that

$$Re = \frac{\bar{u}d}{\nu} < 2300 \quad (2.31)$$

where  $\bar{u}$  is the mean velocity. Above  $Re = 2300$  the mean velocity distribution is likely to be more uniform and the flow is then found to be *turbulent*. Figure 2.5 demonstrates the difference in velocity profiles between laminar and turbulent flow.

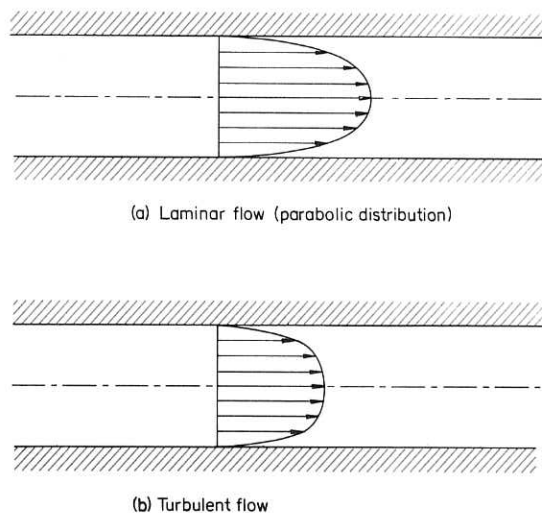


Fig. 2.5 Velocity distributions in a pipe

## 2.6 Turbulent flow

In turbulent flow the fluid particles have a random irregular motion, and at any point in the fluid, their velocity and pressure vary in both time and direction. In any analysis, these physical features of the motion are usually separated into a 'mean component' and a 'fluctuation component', for instance, any mean velocity component and its velocity fluctuation component. This fluctuation affects the mean motion such that there appears an apparent increase in the viscosity of the main flow. The mean velocity components can be shown to satisfy the same equations as those of laminar flow except that the laminar stresses are increased by additional stresses due to turbulent fluctuations; they are known as 'apparent stresses of turbulent flow', or Reynolds stresses. In most flows, the apparent stresses are greater than the viscous components and so the latter may often be omitted.

The no-slip condition means that the mean velocity components must be zero at the wall. The turbulent components also vanish there, and are very small in its vicinity. Accordingly, all components of apparent stress also vanish at the walls and only the viscous stresses of laminar flow are active. It follows that, next to the wall, the viscous stresses predominate over the apparent stresses, and that there should exist a thin layer whose motion is similar to a laminar

one. This is the 'laminar sub-layer'. Since the velocities within it are so small, the viscous forces are dominant and there is no turbulence in it. The laminar sub-layer merges into another layer in which the velocity fluctuations are so great that turbulent shearing

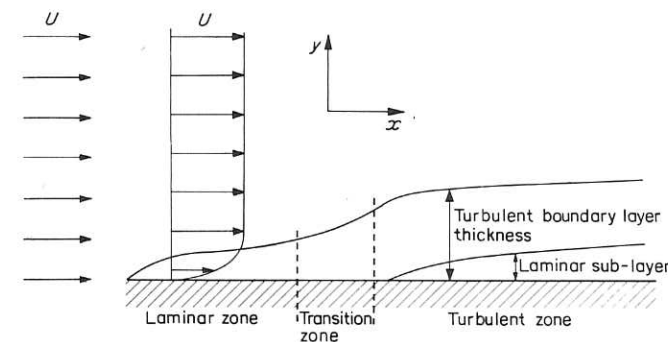


Fig. 2.6 Development of turbulent boundary layer

stresses, comparable to viscous stresses, arise. At larger distances from the wall, the turbulent stresses far exceed the viscous stresses. The turbulent boundary layer is comprised of these distances. The various layers are illustrated in Fig. 2.6 which shows the development of a turbulent boundary layer along a flat plate. At the leading edge, a laminar boundary layer starts to grow. Downstream, a transition region is reached where the flow changes from laminar to turbulent. Beyond this region, the turbulence is fully developed with the laminar sub-layer formed along the wall; and outside the latter layer is the turbulent boundary layer proper. In the next few sections equations will be deduced from which the sizes of the laminar sub-layer and the turbulent boundary layer can be estimated. But first an expression is derived for the pressure gradient down a pipe.

### 2.6.1 Pressure gradient in turbulent flow

We concern ourselves with fully developed turbulent flow down a smooth pipe of diameter  $d$ . The relationship between the pressure gradient and the mean velocity  $\bar{u}$  is usually determined from the laws of friction. To obtain this relationship, it is useful to define a dimensionless coefficient of resistance  $f$ :

$$\left( -\frac{dp}{dx} \right) = \frac{f \rho_e}{2d} \bar{u}^2 \quad (2.32)$$

It is relevant also to introduce here the empirical formula established by Blasius, which relates  $f$  to Reynolds number for smooth pipes of circular cross-section:

$$f = 0.3164 \left( \frac{\bar{u}d}{\nu} \right)^{-1/4} \quad (2.33)$$

where  $\text{Re} = \bar{u}d/\nu$ , and  $\bar{u} = Q/\pi R^2$  where  $Q$  is the volume flow-rate through the pipe. This formula is valid for Reynolds numbers ranging from 3 000 to 100 000.

The pressure drop in turbulent flow is deduced to be:

$$\left( -\frac{dp}{dx} \right) = 0.3164 \frac{\rho_e \bar{u}^2}{2d} \left( \frac{\bar{u}d}{\nu} \right)^{-1/4} \quad (2.34)$$

This equation corresponds to Equations (2.17b) and (2.19). From it, the pressure drop required to overcome viscous forces in turbulent flow can be calculated.

### 2.6.2 Velocity distribution laws

Experimental investigations have demonstrated that for turbulent flow through a smooth pipe, the velocity ratio  $u/u_{\max}$  can be related to the distance ratio  $y/R$  by an empirical expression of the form

$$\frac{u}{u_{\max}} = \left( \frac{y}{R} \right)^{1/n}$$

where  $u$  is the local velocity at distance  $y$ , and  $R$  is the pipe radius. The exponent  $n$  varies with Reynolds number: calculations of the ratio  $u/u_{\max}$  have shown that  $n = 6$  and  $n = 7$  for  $\text{Re} = 4000$  and  $\text{Re} = 100000$ , respectively. Table 2.1 shows the variation in  $n$  as a function of the ratio of mean velocity to maximum velocity.

Table 2.1 Variation in  $n$  as a function of the ratio of mean to maximum velocity in a pipe (after Schlichting [1])

$n$	6	7	8	9	10
$\bar{u}/u_{\max}$	0.791	0.817	0.837	0.852	0.865

On the basis of these dependences and the Blasius formula (2.33), a velocity distribution law can be derived which holds for short distances from the pipe wall. First, the friction velocity,  $u_f$ , is defined:

$$u_f = \left( \frac{\tau_0}{\rho_e} \right)^{1/2} \quad (2.35)$$

where  $\tau_0$  is the shearing stress at the wall of the pipe. Earlier in this section, we noted that inertia forces are negligible in comparison with viscous forces adjacent to the pipe wall. The condition of equilibrium between the force due to the shearing stress  $\tau_0$  on the circumference and the force on the end faces due to the pressure gradient ( $-dp/dx$ ) then is

$$\tau_0 = \left( -\frac{dp}{dx} \right) \frac{R}{2} \quad (2.36)$$

Substitution for ( $-dp/dx$ ) from Equation (2.34) into Equation (2.36) gives

$$\tau_0 = 0.0395 \rho_e \bar{u}^{7/4} \nu^{1/4} d^{-1/4} \quad (2.37)$$

Use of Equation (2.35) then leads to

$$\left( \frac{\bar{u}}{u_f} \right) = 6.99 \left( \frac{u_f R}{\nu} \right)^{1/7} \quad (2.38)$$

The results shown in Table 2.1 now allow the replacement of  $\bar{u}$  by  $u_{\max}$ :  $\bar{u} = 0.8u_{\max}$  for  $n = 7$ . We have

$$\frac{u_{\max}}{u_f} = 8.74 \left( \frac{u_f R}{\nu} \right)^{1/7} \quad (2.39)$$

This equation is usually assumed to hold for any distance  $y$  (and not only  $y = R$ ) and for any velocity  $u(y)$ . That is,

$$\frac{u(y)}{u_f} = 8.74 \left( \frac{u_f y}{\nu} \right)^{1/7} \quad (2.40)$$

Equations (2.39) and (2.40) are based on the Blasius friction factor relationship (2.33) which is valid for Reynolds numbers up to about 100 000 and for values of  $(u_f y/\nu)$  ranging from about 500 to 2000. Above these values, viscous effects no longer predominate

over turbulent stresses and an alternative relationship has to be found. Schlichting [1] quotes the usefulness of these conditions:

Laminar sub-layer:  $0 < u_f y / \nu < 4$  to 5 – only laminar friction exists.

Buffer region:  $4 < u_f y / \nu < 30$  to 70 – laminar and turbulent friction are of the same order of magnitude.

Turbulent region:  $u_f y / \nu > 30$  to 70 – turbulent friction is much greater than laminar friction.

Equations (2.39) and (2.40) indicate that the velocity distribution can be written as a power law. The experimental evidence, that the exponent in those equations decreases as the Reynolds number is increased, suggests that a universal law may exist which is valid for all Reynolds numbers. Such a law, in logarithmic form, has been developed which is applicable, in addition, to other channel flows and to two-dimensional boundary layers. A generally accepted version of the law is

$$\frac{U - u(y)}{u_f} = C_1 \ln \frac{y}{y_0} \quad (2.41)$$

where  $U$  now represents the maximum (centre-line) velocity for pipe flow and the mainstream velocity for boundary layer flow.  $C_1$  is an experimental constant, usually of order  $-2.5$ , and  $y_0$  is some suitable reference length. (Note: in most ECM work,  $U$  and  $\bar{u}$  are regarded as equivalent; both are usually calculated from the volumetric flow-rate at the gap inlet, divided by the cross-sectional area of the channel at inlet.)

### 2.6.3 Thickness of laminar sub-layer

The universal formula allows an expression for the thickness  $\delta_l$  of the laminar sub-layer to be obtained. (This quantity must be known for the calculations of concentration overpotential in the next chapter.) From the condition for the existence of laminar friction in Section 2.6.2,

$$\delta_l \approx \frac{5\nu}{u_f} \quad (2.42)$$

If the velocity  $u(y)$  at the edge of the laminar sub-layer is assumed to be small compared with the mainstream velocity  $U$ , the friction

velocity is given from Equation (2.41) as

$$\frac{U}{u_f} = C_1 \ln \frac{\delta_l}{y_0} \quad (2.43)$$

As always, difficulty arises in the selection of the reference length  $y_0$ . In ECM and for flow down a rectangular channel, a convenient choice for  $y_0$  is the inter-electrode gap width  $h$ . From the discussion in Section 2.1,  $y_0 = 2h$ . By means of Equations (2.42) and (2.43) we deduce that

$$\delta_l = \frac{5\nu C_1}{U} \ln \frac{\delta_l}{2h} \quad (2.44a)$$

(Note: although  $C_1$  is usually about  $-2.5$ , the magnitude of  $\delta_l$  is not greatly affected for  $C_1$  varying between 1 and 10.)

An alternative treatment based on the same reasoning is available [3] which gives the result

$$\frac{\delta_l}{R} = 124 \text{ Re}^{-7/8} \quad (2.44b)$$

where  $R$  is the channel radius and  $\text{Re} = Ud_h/\nu$ , is the Reynolds number.

### 2.6.4 Thickness of the turbulent boundary layer

The exact thickness,  $\delta_t$  of the boundary layer cannot be found since the division between the zones of negligible viscosity and the boundary layer is a gradual one. However,  $\delta_t$  is often defined as the distance at which the velocity reaches an arbitrary percentage fraction of the mainstream velocity (e.g. 99%). This condition is indicated in Fig. 2.7. Two other ‘thicknesses’ can usefully be defined.

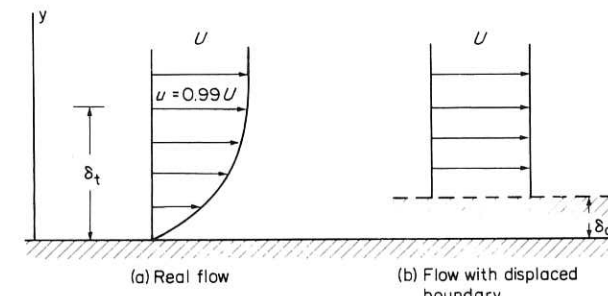


Fig. 2.7 Thickness of turbulent boundary layer

One is the displacement thickness,  $\delta_d$ , the distance by which the boundary would be displaced to maintain the same mass flow at any section, the entire flow being assumed to be frictionless. From Fig. 2.7, by the continuity of mass,  $\delta_d$  is given by

$$\rho_e U \delta_d = \rho_e \int_0^{\delta_t^+} (U - u) dy$$

i.e.

$$\delta_d = \int_0^{\delta_t^+} \left(1 - \frac{u}{U}\right) dy \quad (2.45)$$

where  $\delta_t^+ \geq \delta_t$ .  $U$ , as usual, is the mainstream velocity and  $u$  the velocity within the boundary layer.

A reduction in the momentum flux rate due to the reduction in velocity within the boundary layer gives rise to the 'momentum thickness'  $\theta$ , defined as

$$\rho_e \theta U^2 = \rho_e \int_0^{\delta_t^+} (Uu - u^2) dy$$

or

$$\theta = \int_0^{\delta_t^+} \frac{u}{U} \left(1 - \frac{u}{U}\right) dy \quad (2.46)$$

To illustrate the physical significance of the momentum thickness, a relationship is derived between the shear stress at the boundary and the velocity. From Prandtl's boundary layer equations (2.27) and (2.28), and in the absence of pressure gradient, integration gives

$$\int_{y=0}^{y=\delta_t^+} \left(u \frac{\partial u}{\partial x} + v \frac{\partial u}{\partial y}\right) dy = \nu \int_0^{\delta_t^+} \frac{\partial^2 u}{\partial y^2} dy$$

From Equation (2.1)

$$\mu \int_0^{\delta_t^+} \frac{\partial^2 u}{\partial y^2} dy = \int_0^{\delta_t^+} \frac{\partial \tau}{\partial y} dy = [0 - \tau_0] = -\tau_0$$

Now

$$\begin{aligned} \int_0^{\delta_t^+} v \frac{\partial u}{\partial y} dy &= \int_0^{\delta_t^+} \frac{\partial}{\partial y} (uv) dy - \int_0^{\delta_t^+} u \frac{\partial v}{\partial y} dy \\ &= U v_{\delta_t^+} + \int_0^{\delta_t^+} u \frac{\partial u}{\partial x} dy \end{aligned}$$

by use of the continuity equation and where

$$v_{\delta_t^+} = - \int_0^{\delta_t^+} \frac{\partial u}{\partial x} dy$$

Thus

$$\int_0^{\delta_t^+} u \frac{\partial u}{\partial x} dy - U \int_0^{\delta_t^+} \frac{\partial u}{\partial x} dy + \int_0^{\delta_t^+} u \frac{\partial u}{\partial x} dy = -\frac{\tau_0}{\rho_e}$$

If  $U$  is constant, this equation becomes

$$\frac{\tau_0}{\rho_e} = \frac{\partial}{\partial x} \int_0^{\delta_t^+} u(U - u) dy \quad (2.47)$$

That is,

$$\begin{aligned} \tau_0 &= \rho_e U^2 \frac{\partial \theta}{\partial x} \\ &= \rho_e U^2 \frac{d\theta}{d\delta_t} \frac{d\delta_t}{dx} \end{aligned}$$

Now, from Equations (2.35) and (2.40), and assuming that those analyses for pipe flow can again be applied to flow over a flat plate, we deduce that

$$\tau_0 = 0.0225 \rho_e U^2 \left(\frac{\nu}{U \delta_t}\right)^{1/4} \quad (2.48)$$

The power law derived above can be adapted further. From Equation (2.40),

$$\frac{U}{u_f} = 8.74 \left(\frac{u_f \delta_t}{\nu}\right)^{1/7}$$

and

$$\frac{u(y)}{u_f} = 8.74 \left(\frac{u_f y}{\nu}\right)^{1/7}$$

Combining these equations, we obtain

$$\frac{u(y)}{U} = \left(\frac{y}{\delta_t}\right)^{1/7} \quad (2.49)$$

Substitution for  $u(y)$  and for  $\tau_0$  in Equation (2.48) gives

$$0.0225 U^2 \left( \frac{\nu}{U\delta_t} \right)^{1/4} = \frac{d}{dx} \int_0^{\delta_t} U^2 \left[ \left( \frac{y}{\delta_t} \right)^{1/7} - \left( \frac{y}{\delta_t} \right)^{2/7} \right] dy$$

Integration yields

$$0.0225 \left( \frac{\nu}{U\delta_t} \right)^{1/4} = + \frac{7}{72} \frac{d\delta_t}{dx}$$

Separation of variables and integration again lead to

$$\left( \frac{\nu}{U} \right) x^{1/4} = 3.45 \delta_t^{5/4} + C \quad (2.50)$$

where  $C$  is the constant of integration. This constant is difficult to find, since the turbulent boundary layer starts at the transition zone, downstream from the leading edge; location of that zone is difficult, and moreover, the layer has a finite thickness there. However, it is recognised that if the boundary layer is assumed to start at the edge of the plate, acceptable results can be obtained for points beyond the transition region. If this procedure is followed, and  $\delta_t = 0$  at  $x = 0$ , then  $C = 0$ . Equation (2.50) becomes

$$\delta_t = 0.376 x^{4/5} \left( \frac{\nu}{U} \right)^{1/5} \quad (2.51)$$

## 2.7 Admissible surface roughness

In the above analyses, and in ECM calculations based upon them, the plate and pipe surfaces have been implicitly assumed to be hydraulically smooth. Some surface roughness is usually thought to be tolerable, so that the condition for hydraulic smoothness can still be maintained, provided the height of the roughness irregularities is below a critical amount. This amount also appears to depend on the type of flow.

For turbulent flow along a pipe and a flat plate, one recommended relationship is

$$\frac{U\epsilon_{adm}}{\nu} = 10^2 \quad (2.52)$$

where  $U$  is the mainstream velocity,  $\epsilon_{adm}$  is the admissible height of the surface projections, and  $\nu$  is the kinematic viscosity. The follow-

ing corresponding relationship for laminar flow has also been suggested:

$$\frac{u_f \epsilon_{adm}}{\nu} = 15 \quad (2.53)$$

where  $u_f$  is the friction velocity, Since

$$u_f = \left( \frac{\tau_0}{\rho_e} \right)^{1/2} \quad (2.35)$$

It can also be shown that the shearing stress  $(\tau_0/\rho_e)$  is given by

$$\frac{\tau_0}{\rho_e} = 0.332 U^2 \left( \frac{\nu}{Ux} \right)^{1/2} \quad (2.54)$$

[cf. Equation (2.48) for turbulent flow]. Hence,  $\epsilon_{adm}$  can be expressed in terms of  $U$ ,  $\nu$ ,  $\rho_e$ , and  $x$ .

The usefulness of these hypotheses remains to be tested in ECM work. Nevertheless, it has been claimed that, because of the small hydraulic diameter of the flow channel in ECM, even optically smooth surfaces can act as rough surfaces [4].

## 2.8 Separation

In many ECM applications, flow over curved surfaces is more likely than flow over flat ones. With the former kind of flow, a phenomenon called 'separation' may arise.

Consider a fluid passing over a gently curved body, as indicated in Fig. 2.8. Upstream, between points A and B, the mainstream velocity just outside the boundary layer increases continually. From Bernoulli's equation, it is clear that this rate of increase of velocity must be accompanied by a decrease in pressure. Downstream, beyond point C, a corresponding decrease in mainstream velocity and increase in pressure take place. That is, at a stage between B and C, the fluid within the boundary layer is affected by a pressure which increases in the direction of flow, normally called the 'adverse pressure gradient'. Consequently, the fluid velocity may be reduced. If the velocity eventually becomes zero and then reverses direction, the boundary layer will be 'separated' from the body.

A necessary condition for separation can be derived from Prandtl's boundary layer equations; in terms of Fig. 2.8,  $x$  is now regarded

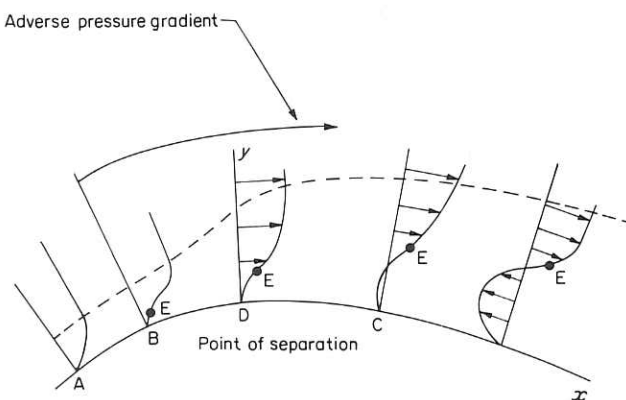


Fig. 2.8 Development of separation

as a curvilinear coordinate along the line of the boundary, and  $y$  is the normal distance from the boundary.

Suppose that separation starts at point D, at which the velocity and its variation in the  $y$  direction are zero. That is, at D,

$$\left(\frac{\partial u}{\partial y}\right)_{y=0} = 0 \quad (2.55)$$

But, at D also,  $u = v = 0$ . So

$$\frac{1}{\rho_e} \frac{dp}{dx} = \nu \left( \frac{\partial^2 u}{\partial y^2} \right)_{y=0} \quad (2.56)$$

First, for  $dp/dx < 0$  (flow conditions between A and B), we see that  $\partial^2 u / \partial y^2 < 0$  near the boundary. In the direction towards the mainstream, the velocity approaches the local mainstream asymptotically, and accordingly, the rate of decrease of  $\partial u / \partial y$  is also reduced. Then, near the edge of the boundary layer,  $\partial^2 u / \partial y^2 < 0$ . Therefore, the curvature of the velocity profile is always negative for decreasing pressure.

Next, for  $dp/dx > 0$ ,  $\partial^2 u / \partial y^2 > 0$ . But, flow conditions near the edge of the boundary layer have not altered, and there  $\partial^2 u / \partial y^2 < 0$ . It is deduced that an inflexion point in the profiles must exist; its position is indicated by E in Fig. 2.8.

On the boundary at the point of separation,  $\partial u / \partial y = 0$ . Since the velocity increases continuously from zero at the boundary and eventually to some positive value adjacent to the boundary, we infer that  $\partial^2 u / \partial y^2 > 0$ . But, at the edge of the boundary layer,  $\partial^2 u / \partial y^2 < 0$ ,

so that a point of separation must be associated with an inflection point, and hence with an adverse pressure gradient.

Finally, we add that separation can also occur if the entry to the flow channel is abrupt. Also, in the wake downstream from the separation point, eddies and vortices are generated. Some effects which they appear to have on surface finish in ECM are discussed in Chapter 4.

## 2.9 Utilisation of fluid dynamic principles in ECM

Considerations of flow phenomena in ECM are usually based on the principles outlined in the above sections. The purpose of this section is to show examples of their use.

An important feature required for accurate study of fluid flow in ECM is that of an inlet length to provide fully developed velocity profiles between the electrodes. From Section (2.3.2), this inlet length is about 30 (laminar flow) to 100 (turbulent flow) pipe diameters. Its inclusion means that the inlet pressure has to be increased, often quite drastically. In practice, this increase is sometimes not possible, and hydrodynamic inlet lengths are often omitted, particularly in industrial ECM operations.

But many experimental ECM apparatuses do carry inlet lengths. One system has been described [5] which provided linear flow-rates between 1 and 25 m/s between rectangular electrodes of side 0.53 by 3.17 mm (smaller dimension in the direction of flow). In the cell, the electrolyte was forced down a rectangular channel of 0.5 × 8 mm cross section and 120 mm length, and the flow channel carried a hydrodynamic inlet length of 77 hydraulic diameters to ensure a fully developed velocity profile at the electrodes. The maximum pressure at the cell inlet was about 10<sup>3</sup> kN/m<sup>2</sup> which yielded a volume flow-rate of 10<sup>-4</sup> m<sup>3</sup>/s through the cell.

The electrode dimensions in that work were made much smaller than those normally met in ECM in order that carefully controlled experiments could be performed. In another investigation [6] rectangular electrodes of size 102 by 12.55 mm have been used (larger dimension in the flow direction) with an inlet length of 78 hydraulic diameters incorporated into the cell to provide fully established flow. Although these electrode dimensions are more likely in ECM, the electrode gap width in that work was 3.175 mm, which is greater than that usually found. Nonetheless, some

characteristic data can be obtained from it. First, the hydraulic mean diameter [Equation (2.4)] is calculated:

$$d_h = \frac{4A}{C} = \frac{4 \times (3.175 \times 12.55)}{2(3.175 + 12.55)} = 5.06 \text{ mm}$$

Note that here the approximation (2.5) cannot be used. The Reynolds number,  $Re$ , can now be found from Equation (2.3), in which the characteristic length is given by the hydraulic diameter:

$$Re = \rho_e \frac{\bar{u} d_h}{\mu} = 7740$$

where  $\rho_e = 1.09 \text{ g/cm}^3$  and  $\mu = 1.19 \text{ cP}$ . [In this calculation, a value for the average velocity has been found from the volumetric flow-rate  $Q$ , as suggested in Section 2.3.2:  $\bar{u} = Q/A = (0.0666 \times 10^{-3})/(39.8 \times 10^{-6} = 1.67 \text{ m/s})$ .] Since  $Re > 2300$  [Equation (2.31)], the flow can be regarded as turbulent.

These values have been used to estimate the viscous pressure drop down the channel for turbulent flow [Equations (2.32), (2.33), and (2.34)]. The friction factor  $f$  is first found:

$$f = \frac{0.3164}{Re^{1/4}} = 0.0337$$

The pressure drop is now given by

$$\frac{fL\rho_e \bar{u}^2}{2d_h} = 1.03 \text{ kN/m}^2$$

where  $L$  is the electrode length ( $= 102 \text{ mm}$ ).

Two other calculations are of interest. First, the thickness of the laminar sub-layer is found from Equation (2.44b):

$$\delta_1 = 124 R(Re)^{-7/8} = 0.12 \text{ mm}$$

where  $R = d_h/2$ .

The corresponding thickness of the turbulent boundary layer is [Equation (2.51)]:

$$\begin{aligned} \delta_t &= 0.376 x^{4/5} \left( \frac{\nu}{U} \right)^{1/5} \\ &= 3.5 \text{ mm} \end{aligned}$$

where  $\delta_t$  is calculated at  $x = L$  ( $= 102 \text{ mm}$ ),  $\nu = 1.091 \text{ mm}^2/\text{s}$ ,  $U(\equiv \bar{u})$  now)  $= 1.67 \text{ m/s}$ .

For interest, a hypothetical laminar boundary layer thickness is calculated from the same data:

$$\delta_0 = 5 \left( \frac{\nu x}{U} \right)^{1/2} = 1.29 \text{ mm}$$

With this hypothetical case, the thickness of the laminar boundary layer is seen to be less than that of the turbulent layer.

Estimates have been made [7] of the laminar boundary layer thickness over the inlet region of a 'quasi-rectangular' channel with gap widths of 0.1 to 0.5 mm and channel length of 2 mm. Equation (2.25) has been used to obtain this thickness, a numerical coefficient of three instead of five being used. For velocities in the range 0 to 9 m/s and for  $\nu \approx 1 \text{ mm}^2/\text{s}$  the estimated thickness is always less than half the gap width even at the exit. It is deduced that fully developed flow does not occur anywhere along this length of channel.

In a practical ECM cell the gap width is usually much less than breadth and length of the electrodes, which latter quantities can be large (e.g. 100 mm). The flow is usually turbulent. It is often useful to have an idea of the minimum pressure required to maintain a required flow-rate down the channel. We can find this amount for flow down a rectangular channel from Equations (2.30) and (2.17b) (laminar flow) or (2.34) (turbulent flow).

#### Example

These formulae have been applied to a case in which electrolyte of density  $\rho_e = 1.088 \text{ g/cm}^3$  and viscosity  $\mu = 0.876 \text{ cP}$  has been pumped at a volume flow-rate of  $0.98 \times 10^{-3} \text{ m}^3/\text{s}$  between rectangular parallel electrodes of area  $76.2 \times 38.1 \text{ mm}^2$  their gap distance at inlet being 0.92 mm.

The mean velocity is calculated to be 27.96 m/s and the Reynolds number 64 000 with  $d_h = 2h = 1.84 \text{ mm}$ . The friction factor ( $f = 0.3164/Re^{1/4}$ ) is calculated to be 0.0199. The dynamic pressure, all of which is assumed to be lost at exit from the channel, is now estimated to be

$$0.5 \rho_e \bar{u}^2 = 420 \text{ kN/m}^2$$

The pressure needed to overcome friction effects is

$$\frac{1}{2} \frac{f \rho_e L \bar{u}^2}{d_h} = 350 \text{ kN/m}^2$$

Thus the total minimum pressure required to force the electrolyte down this channel is estimated to be  $770 \text{ kN/m}^2$ . In practice, the actual pressure drop without ECM was found to be  $613 \text{ kN/m}^2$ . The discrepancy can be attributed to a possible difference between the calculated friction factor and the experimental one, and to the neglect of other possible hydrodynamic factors (e.g. cavitation – see below – which might have affected the friction loss calculations). But the calculations do demonstrate their usefulness in providing a minimum value for the required pressure. With ECM the required pressure will be increased even more.

### 2.10 Multi-phase flow

The generation of gas at the electrodes, particularly cathodic hydrogen, and the dissolution of metal from the anode, mean that the fluid in the machining gap in ECM is of a multi-phase, rather than a single-phase, nature.

In most investigations of fluid flow in ECM, only the gas bubbles are assumed to have appreciable effect on the nature of the flow, which therefore can be regarded as two-phase. The pattern of two-phase flow is determined by the bubble (or void) distribution, an understanding of which usually also demands knowledge of the velocity and shear distributions of the flow. Such information is often difficult to find. Nonetheless, with two-phase flow, certain typical phenomena can arise, and in this section some which are relevant to ECM are briefly described.

#### 2.10.1 Effect on pressure drop

Although this aspect of two-phase flow on the ECM process is also considered in Chapter 5, one feature can usefully be introduced here, namely, the effect on the pressure drop for rectangular channel flow. In Fig. 2.9 are shown pressure drop measurements for a 10% NaCl solution flowing down a channel of length 152 mm, breadth 25 mm, and (gap) width 3.2 mm. The pressure drop without ECM can be estimated from Bernoulli's equation and the Blasius relation given above (for turbulent flow). For flow with ECM, a higher pressure drop is required to maintain the same volume flow-rate of solution, and this increase in pressure drop itself becomes greater at the higher rates of ECM, and becomes less with the higher pressures at outlet to the gap.

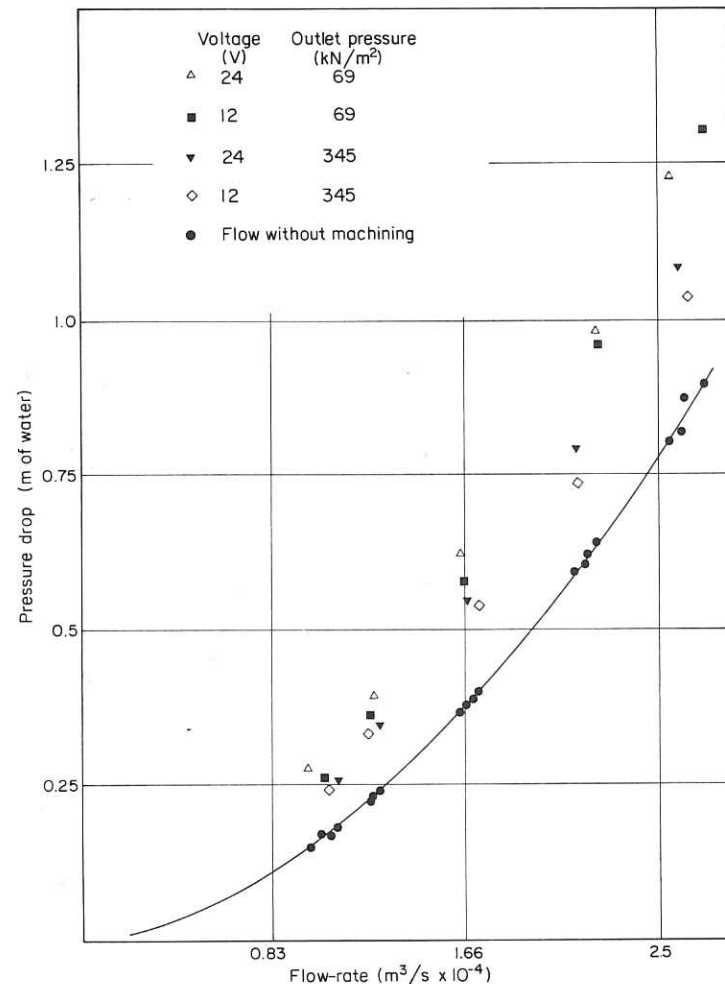


Fig. 2.9 Pressure drop without ECM and with ECM (after Clark [6])

#### 2.10.2 Choking flow

The presence of gas in the electrolyte solution in ECM means that 'choking', a phenomenon associated with compressible fluid flow, could arise. The characteristics of choking can be illustrated from considerations of one-dimensional flow down a duct.

First, consider the flow of an incompressible fluid which starts from rest in a large reservoir of high pressure. Since the density of the fluid is constant and if the mass flow-rate is also assumed to be constant, the velocity will rise continuously as the channel area

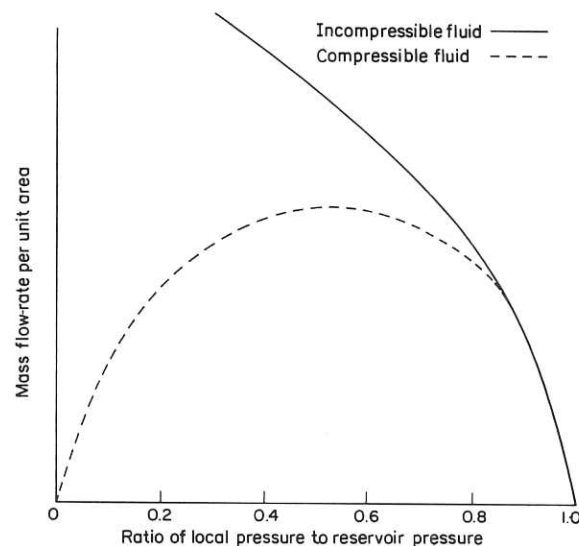


Fig. 2.10 Variation of mass flow rate per unit area with pressure for an incompressible and a compressible-fluid (e.g. air), expanded isentropically

decreases and as the pressure falls to zero. The mass flow-rate per unit area will also rise continuously with falling pressure. The maximum velocity, and hence mass flow-rate, can, of course, be found from Bernoulli's equation.

On the other hand, for a compressible fluid, it can be shown that as the pressure falls the mass flow-rate per unit area first increases. But the mass flow-rate, after reaching a maximum value, decreases as the density decreases. This maximum is determined only by conditions in the reservoir and by the smallest area of the duct. This condition is referred to as *choking*. This critical mass flow-rate cannot be increased further by further change in differential pressure along the length of the channel. The variation of mass flow-rate per unit area with pressure for both an incompressible and a compressible fluid is shown in Fig. 2.10.

### 2.10.3 Cavitation

As the electrolyte solution flows between the electrodes during ECM, its temperature will rise owing to, for example, the passage of current and the pressure drop along the flow channel. This increase can lead to the growth of gas-filled bubbles (cavities). If the growth of the bubbles is caused by temperature increase, boiling occurs. If

their growth is due to pressure reduction (at constant temperature) 'cavitation' is said to have occurred.

Studies of cavitation relate to (i) the formation of bubbles in the liquid caused by reductions in pressure below certain critical values, determined by the physical condition of the liquid, and (ii) the collapse of bubbles due to an associated increase in pressure. Cavitation behaviour is known to take place either in the bulk of the liquid or at its interface with a boundary, and the presence of cavities can lead to displacement of the liquid phase of the solution, causing alteration in the flow pattern. A further effect can be damage to the channel walls. Suppose that, during ECM, the pressure conditions and the configuration of the electrodes lead to the formation of cavities which are later swept by the flow into regions of higher pressure where the cavities collapse. If the point of collapse of cavity is in contact with either of the electrodes, the wall of the electrode will receive a blow. The consequence of successive blows may be damage to the electrode material.

In ECM cavitation is more likely to arise at a location where an abrupt change occurs in the direction of flow, associated with which is a sudden decrease in the local pressure. The problem has been the subject of a number of investigations [8, 9]. In one study of electrochemical die-sinking, the electrolyte was pumped through a central nozzle and then outwards in a radial direction. Calculations, based on Bernoulli's equation and the equation for the pressure drop caused by viscous effects, showed that pressures near the nozzle inlet could be less than the vapour pressure of the electrolyte, indicating that cavitation was likely in that region. This was confirmed by experiment. It was also found that the onset of cavitation could be prevented by the application of a sufficiently high outlet or 'back' pressure. Cavitation was also eliminated when the electrolyte was caused to flow in the reverse direction. The shape of the nozzle also played an important role: a sharp-cornered nozzle required a higher limiting outlet pressure to eliminate cavitation than did a smoothly tapered nozzle. (No quantitative information is available to support this observation. Presumably a sharp-cornered nozzle caused the flow direction to change abruptly, with a correspondingly abrupt decrease in pressure. These conditions would then be more favourable to cavitation.)

Figure 2.11 shows another configuration of electrodes used to study cavitation in ECM [10]. The electrodes are plane and parallel

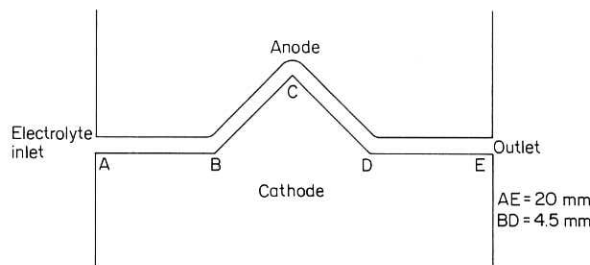


Fig. 2.11 Configuration of electrodes for investigation of cavitation in ECM (after Ito and Seimiya [10])

along the length AB whilst along BCD the cathode is in the shape of a right-angled wedge. A 10% (w/w) NaCl solution was forced down the gap at Reynolds numbers ranging from 8 000 to 20 000, the pressure at inlet being  $1570 \text{ kN/m}^2$  and the outlet pressure being varied from  $980$  to  $1170 \text{ kN/m}^2$ .

Cavitation bubbles are seen as the white layer at the top of the wedge portion of the cathode in Fig. 2.12. The amount of cavitation

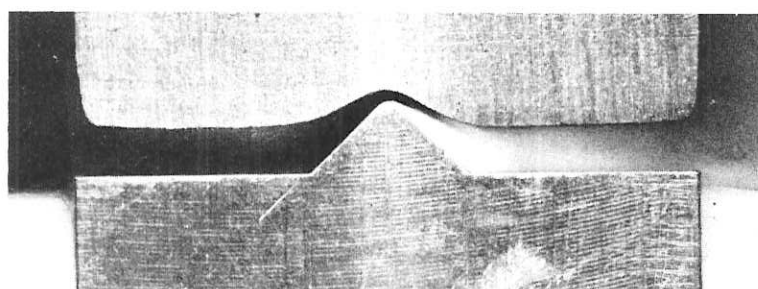


Fig. 2.12 Cavitation during ECM (voltage = 15 V; feed-rate =  $0.02 \text{ mm/s}$ ; outlet pressure =  $294 \text{ kN/m}^2$ ) (By permission of S. Ito and K. Seimiya [10])

could again be reduced by increasing the outlet pressure. For the conditions given above, cavitation was eliminated when the outlet pressure was about  $780 \text{ kN/m}^2$ .

Cavitation will be discussed later in connection with surface finish and limitations on the rate of ECM.

## References

1. See, for example, Schlichting, H., *Boundary Layer Theory*, McGraw-Hill, New York (1968).
  2. See, for example, Chin, D. T., *J. Electrochem. Soc.* (1972) **119**, No. 8, 1043.
  3. Knudsen, J. G. and Katz, D. L., *Fluid Dynamics and Heat Transfer*, McGraw-Hill, New York (1958).
  4. Tobias, C. W., Paper presented at First Int. Conf. on ECM, Leicester University, March 1973.
  5. Landolt, D., Muller, R. H. and Tobias, C. W., *J. Electrochem. Soc.* (1969) **116**, No. 10, 1384.
  6. Clark, W. G., Ph.D. Thesis, Strathclyde University, Glasgow (To be submitted).
  7. Kruissink, C. A., Paper presented at First Int. Conf. on ECM, Leicester University, March 1973.
  8. Chikamori, K., Ito, S. and Sakurai, F., *Bull. Jap. Soc. Prec. Eng.* (1968) **2**, No. 4, 318.
  9. Ito, S., Chikamori, K. and Sakurai, F., *J. Mech. Lab. Japan* (1966) **12**, No. 2, 37.
  10. Ito, S. and Seimiya, K., *Proc. 12th Int. Conf. Mach. Tool Res.*, Macmillan (1972) p. 259.
- ## Bibliography
- Knapp, R. T., Daily, J. W. and Hammitt, F. G., *Cavitation*, McGraw-Hill, New York (1970).  
 Knudsen, J. G. and Katz, D. L., *Fluid Dynamics and Heat Transfer*, McGraw-Hill, New York (1958).  
 Schlichting, H., *Boundary Layer Theory*, McGraw-Hill, New York (1968).  
 Shames, I. H., *Mechanics of Fluids*, McGraw-Hill, New York (1962).  
 Tong, L. S., *Boiling Heat Transfer and Two-Phase Flow*, Wiley, New York (1965).  
 Wallis, G. B., *One Dimensional Two-Phase Flow*, McGraw-Hill, New York (1969).